THE JOURNAL OF PHYSICAL CHEMISTRY B

Article

Cite This: J. Phys. Chem. B 2018, 122, 8462−8468

pubs.acs.org/JPCB

Inverse Design of Colloidal Crystals via Optimized Patchy Interactions

D. Chen,[†] G. Zhang,[†] and S. Torquato*[,†,‡,§,∥]

[†]Department of Chemistry, [‡]Department of Physics, [§]Princeton Institute for the Science and Technology of Materials, and [∥]Program in Applied and Computational Mathematics, Princeton University, Princeton, New Jersey 08544, United States

ABSTRACT: Inverse statistical mechanics is a powerful optimization methodology that has been widely applied to design optimal isotropic pair interactions that robustly yield a broad spectrum of target many-particle configurations or physical properties. In this work, we generalize inverse techniques to design experimentally realizable spherical colloidal particles with optimized "patchy" anisotropic interactions for a wide class of targeted low-coordinated two-dimensional crystal structures that are defect-free. Our target crystals include square, honeycomb, kagomé, and parallelogrammic crystals. The square, honeycomb, and kagomé crystals possess desirable photonic, phononic, and magnetic properties, which are useful for a wide range of applications. We demonstrate that these target configurations can be robustly achieved with relatively few defects at sufficiently low temperatures. Our findings provide experimentalists with the optimal parameters to synthesize these crystals with patchy colloids under standard laboratory conditions.

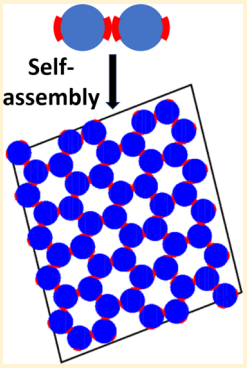

I. INTRODUCTION

More than a decade ago, Rechtsman, Stillinger, and Torquato initiated the inverse statistical mechanics approach to design optimal isotropic pair interactions that yield novel target crystal structures as ground states.[1−3] It was demonstrated that such inverse optimization methods could robustly stabilize low-coordinate crystal structures, such as the honeycomb[1,2] and square[2] lattices in two dimensions and the simple cubic lattice in three dimensions.[3] In this inverse approach, a target many-particle configuration in d-dimensional Euclidean space $\mathbb{R}^d$ or a target physical property is first specified, and then one attempts to find a parameterized total potential energy $\Phi(\mathbf{r}^N)$ under certain constraints that achieve the targeted behavior(s),[1] where $\mathbf{r}^N = \mathbf{r}_1, \mathbf{r}_2, ..., \mathbf{r}_N$ denotes the configurational coordinates of N particles within a fundamental cell under periodic boundary conditions. This inverse procedure is to be contrasted with the conventional forward approach,[4−8] where one first specifies the total potential $\Phi(\mathbf{r}^N)$ and then probes the structures in its phase diagram.

Since 2005, a variety of different groups have adopted this inverse approach to design novel targeted many-particle configurations with desirable bulk physical properties through the use of isotropic pair potentials.[2,3,9−21] These structures include low-coordinated crystals as ground states (such as the kagomé, rectangular, and rectangular kagomé crystals in $\mathbb{R}^2$ (see refs 12, 13, and 17) and diamond, wurzite, and CaF_2 crystals in $\mathbb{R}^3$ (see refs 9, 16, and 17), and those with excited-state properties (such as negative thermal expansion[10] and negative Poisson ratio[11]). These findings demonstrated the surprisingly rich capacity of isotropic pair potentials to stabilize a broad class of structures. However, experimental realization of such interactions remains challenging because they generally possess complex functional forms.

Anisotropic pair interactions offer greater flexibility to achieve targeted structures both theoretically as well as experimentally. However, the application of inverse methods to optimized directional (anisotropic) interactions is still in its infancy. We are aware of only one such previous work due to Escobedo,[22] which involves nonspherical particles and anisotropic interactions that were optimized over a single parameter.

Here, we extend our inverse approach to design many-particle systems of spherical colloidal particles with optimized "patchy" anisotropic interactions. As a proof-of-concept, we consider a wide class of targeted low-coordinated crystals in two dimensions that are defect-free. Obtaining defect-free versions of these crystals is nontrivial and requires a delicate search of the parameter space. A major motivation for this study is that patchy colloidal particles can be readily fabricated in experiments and have been shown to be able to self-assemble into a variety of interesting structures.[23−32] For example, in a pioneering work, Chen et al.[28] synthesized colloidal particles that self-assembled into a four-coordinated kagomé crystal with electrostatic repulsion in the middle and hydrophobic attraction at the two pores. Romano and Sciortino[29] subsequently reproduced these experimental findings via computer simulation by modeling the particles as hard spheres with two attractive patches. Such spheres were constrained to move on a flat surface, but nonetheless could rotate freely in three dimensions.[29]

We consider technologically relevant two-dimensional (2D) target crystals, including the square, honeycomb, kagomé, and parallelogrammic crystals. The honeycomb and kagomé crystals possess desirable photonic band gap properties, which are useful

Received: June 12, 2018
Revised: July 22, 2018
Published: August 8, 2018

DOI: 10.1021/acs.jpcb.8b05627
J. Phys. Chem. B 2018, 122, 8462−8468

for applications, such as waveguides, optical circuits, and other photonic devices.[1,33,34] The square and honeycomb crystals also possess complete phononic bandgaps,[35] and the kagomé crystal is a promising magnetic material, since it naturally leads to spin-frustration when the system contains antiferromagnetic interactions.[36] We show that these target crystals can be realized with relatively few defects at sufficiently low, yet experimental realizable temperatures (not necessarily ground states).[28] Moreover, we demonstrate that our 2D target structures can be robustly achieved in the laboratory by depositing particles onto a surface and then allowing them to self-assemble into target crystals within the plane. In the cases of kagomé and parallelogrammic crystals, experimental realization can be achieved by creating net surface charges at specific sites of the particle surfaces.

The rest of the paper is organized as follows: in Section II, we describe how we adapt the inverse statistical mechanics approach to the general case of anisotropic patchy potentials. In Section III, we present our optimized parameters for the robust assembly of 2D square, honeycomb, kagomé, and parallelogrammic crystals. We offer concluding marks and discussion in Section IV.

II. METHODS

A. General Scheme of Inverse Statistical Mechanics Approach. In a previous work, Zhang, Stillinger, and Torquato developed an improved inverse statistical mechanics approach.[17] Specifically, they fix the pressure p rather than the specific volume $v = V/N$ of the system, where N is the number of particles and V is the volume. At constant p and N, the classical ground state is achieved by the global minimum of the configurational enthalpy per particle

$$h(\mathbf{r}^N) = \Phi(\mathbf{r}^N)/N + pv \tag{1}$$

This approach minimizes the occurrence of encountering phase separation and allows the box to fully deform such that no symmetries of the box are imposed, which facilitates finding the true enthalpy-minimizing structure during the simulations.[17]

As a first step, a list of competitor structures associated with the target structure is identified by running many instances of forward simulations. Next, an objective function and the nonlinear "Subplex" optimization algorithm[37] are carefully chosen to obtain optimal potential parameters and pressure that favor the target structure over its competitors. In particular, the objective function in ref 17 involves the product of the curvature of the enthalpy surface around the target structure and the enthalpy difference between the target structure and the lowest minimum (except the target structure) of the enthalpy surface. The choice of this objective function is essential for the robust self-assembly of some of the complex target structures reported there.

B. Inverse Approach for Patchy Interactions. In the context of patchy interactions, it is difficult to find an appropriate objective function, such as the ones used in previous works,[1,16,17] since the family of patchy potentials contain a singular hard-core interaction and are discontinuous radially and angularly (see Section III for detailed functional forms of the potential). Therefore, a full-blown optimization of the parameters for given target crystals is practically very challenging to carry out through the use of standard optimization algorithms. Given this technical difficulty, we instead search the parameter space of p, θ, and λ in a discrete manner via a multistage grid-search approach to determine the optimal values. Specifically, we first use a large grid to search a large portion of the parameter space. For each set of parameter values, we run a forward simulated annealing to determine the corresponding low-temperature equilibrium structure formed by the self-assembly of the patchy particles, as detailed below in Section II(C). Afterward, we visually inspect all of the resulting structures, and then proceed to the next stage and use a smaller grid to search in the vicinity of the promising candidate values found in the previous stage. We repeat this process and gradually reduce the grid size until we find a set of parameter values that lead to relatively defect-free target crystals. By "relatively defect-free", we mean obtaining perfect crystals for small system sizes (typically for $N \leq 100$) and crystals with less than 5% vacancy defects for larger system sizes. The grid size (or resolution) used for the search over the parameters may generally be different from one another.

In particular, to determine optimal pressure p for a given target crystal, we generally start with a grid size of 0.50 within the range of $[0, 2.50]$ in the units of ϵ/σ^2, where ϵ is the energy scale of the potential and σ is the diameter of the particle. We then employ a smaller grid size of 0.10 in the vicinity of the promising candidate values found in the first stage if necessary. The grid size continues to be decreased to smaller values (e.g., 0.01), if we fail to obtain relatively defect-free target structures in the previous stages. At each fixed p, if the resulting structure is one with large voids, we need to increase p; on the other hand, if the resulting structure is a highly-coordinated one, like the triangular lattice, p needs to be lowered. For other parameters in the patchy potential, one stage of a grid search with a fine grid is generally sufficient to find optimal values since the resulting structures are not very sensitive to these parameters. Specifically, we employ a grid size of 0.05 and $\pi/12$ for the search of optimal λ and θ, respectively. Moreover, we find that the structures essentially remain unchanged with respect to variations of θ within certain small intervals, consistent with ground-state degeneracy found in previous works.[38−40]

C. Procedure for Obtaining Low-Temperature Structure of a Given Patchy Potential. We employ the simulated annealing Monte Carlo approach[17] to obtain the low-temperature equilibrium structure of a given patchy potential. We apply periodic boundary conditions and set the initial shape of the simulation box to be a square. We start with random initial configurations. At each step, a trial move can be a small random displacement or rotation of a randomly selected particle or a small random deformation of the simulation box, with the probabilities of occurrence of these three events given by p_v, p_r, and p_b. We set $p_b = 1/(5N - 4)$ and $p_t = p_r = (1.0 - p_b)/2$, where N is the number of particles in the system. The trial move is accepted with probability

$$p_{acc}\ (\text{old} \rightarrow \text{new}) = \min\left\{1, \exp\left(-\frac{H_{new} - H_{old}}{k_B T}\right)\right\} \tag{2}$$

where k_B is the Boltzmann's factor, T is the temperature of the system that is set initially high and gradually decreases according to a cooling schedule, and H_{old} and H_{new} are the enthalpies of the system before and after the trial move. Here, we employ the "thermodynamic cooling schedule" with a dimensionless thermodynamic speed $v_s/\sqrt{k_B} = 2.5 \times 10^{-5}$,[41] which automatically sets the number of Monte Carlo moves at each temperature stage. Trial moves are repeated until the temperature T drops below a threshold value, which we set as $k_B T/\varepsilon = 0.1$. This termination temperature is achievable under standard

DOI: 10.1021/acs.jpcb.8b05627
J. Phys. Chem. B 2018, 122, 8462−8468

laboratory conditions. Note that due to the discontinuous nature of the potential, when the kinetic energy k_BT is much smaller than the energy scale ε of the attractive part of the patchy potential, the equilibrium structure of the system is essentially the same as the ground state.

III. RESULTS

We start with the following parameterized interaction due to Kern and Frenkel[23,29]

$$\Phi(\mathbf{r}^N) = \sum_{i<j}^{N} u_2(\mathbf{r}_{ij}) \tag{3}$$

where $u_2(\mathbf{r}_{ij})$ is given by

$$u_2(\mathbf{r}_{ij}) = \begin{cases} \infty, & \text{if } r_{ij} < \sigma \\ -\varepsilon, & \text{if } \sigma < r_{ij} < \lambda\sigma,\ \hat{\mathbf{n}}_i\cdot\hat{\mathbf{r}}_{ij} \geq \cos\theta \\ & \text{and } \hat{\mathbf{n}}_j\cdot\hat{\mathbf{r}}_{ji} \geq \cos\theta \\ 0, & \text{otherwise} \end{cases} \tag{4}$$

$\mathbf{r}_{ij}$ is the vector from the center of particle i to that of particle j, $r_{ij} \equiv |\mathbf{r}_{ij}|$, $\hat{\mathbf{r}}_{ij} \equiv |\mathbf{r}_{ij}|/r_{ij}$, $\hat{\mathbf{n}}_i$ is the unit normal vector of the patch on particle i that is closest to particle j, σ is the diameter of the hard core, and λ and θ are the radial range and the half angular width of the patches, respectively. This type of patchy particle interaction is illustrated in Figure 1 and subsequently we will probe its limitation in terms of generating 2D crystals.

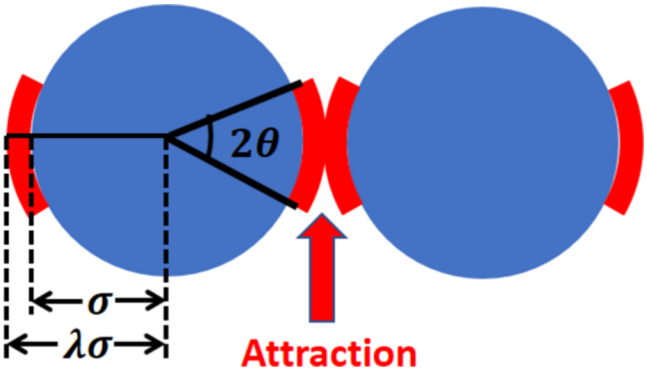

Figure 1. Illustration of the patchy interactions given by eq 4, where the repulsive cores and attractive patches of the particles are colored blue and red, respectively. In this example, each particle has two patches equally spaced (180° apart) over the surface of the particle. The angular width and radial range of the patches are given by 2θ and λ, respectively.

Subsequently, we tune the parameters λ, θ, and the pressure p to obtain the aforementioned targeted relatively defect-free crystals in simulations. For the simple square crystal, we use four identical patches centered at the angles consistent with the tetravalent coordination of this crystal. For each choice of λ, θ, and p, we perform simulated annealing[17] of a system with $N = 64$ particles (see detail of the simulated annealing procedure in Section II). We find that when $\lambda = 1.05$, $\theta = \pi/12$, and $p = 1.20$, the particles self-assemble into a perfect simple square crystal, as shown in Figure 2a. The corresponding effective packing fraction of the colloids (the fraction of space covered by the hard cores of the colloids) ϕ is 0.75. We also study a larger system with $N = 225$ particles and are able to obtain a square crystal with only a few vacancy defects (a vacancy percentage less than 5%)

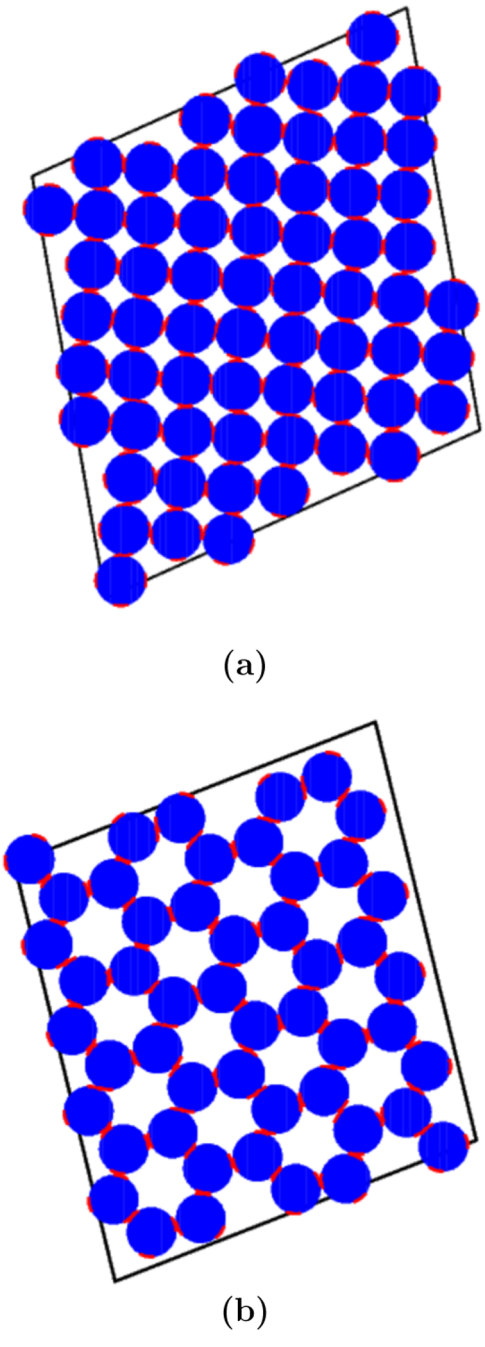

Figure 2. (a) Self-assembly of perfect simple square lattice by particles with hard cores and four attractive equally-spaced patches over each particle. The optimized parameters are found to be $\lambda = 1.05$, $\theta = \pi/12$, and $p = 1.20$. (b) Self-assembly of perfect honeycomb lattice by particles with hard cores and three attractive patches equally spaced on each of the particles. The optimized parameters are found to be $\lambda = 1.05$, $\theta = \pi/12$, and $p = 0.42$.

via simulated annealing. We note that the presence of defects could be due to kinetic trapping in Monte Carlo simulation, as mentioned elsewhere.[19] This does not necessarily occur in experiments, which can usually access much larger time scales. The few defects found in our simulations likely arise because we are considering equilibrium structures at low temperatures (not ground states) where thermal excitations induce defects.

For the honeycomb crystal, we employ similar procedures as those for the square crystal, except that we use $N = 50$ particles

DOI: 10.1021/acs.jpcb.8b05627
J. Phys. Chem. B 2018, 122, 8462−8468

and three identical patches equally spaced on the surface of each particle, which is consistent with the trivalent coordination of this crystal. We find that when $\lambda = 1.05$, $\theta = \pi/12$, and $p = 0.42$, the particles self-assemble into a perfect honeycomb lattice, as shown in Figure 2b. The corresponding effective packing fraction of the colloids ϕ is 0.58.

For the kagomé crystal, we first attempt to employ particles with two identical patches,[29] but only allow the particles to rotate within the plane. However, we find that at different pressures, the resulting structures are dense triangular crystal (as shown in Figure 3), which is a competitor structure favored over

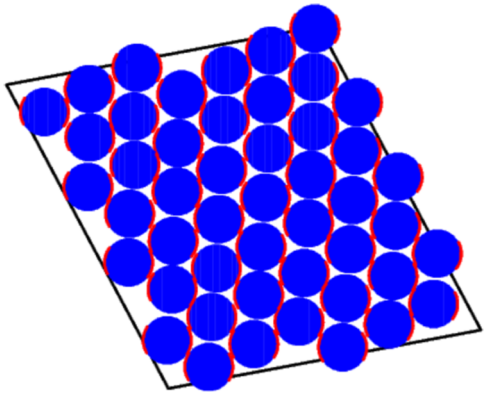

Figure 3. Representative configuration of a dense triangular crystal by the self-assembly of particles with hard cores and two attractive equally-spaced patches over each particle. Importantly, this is a competitor structure favored over the target kagomé crystal at different pressures.

the desired kagomé crystal. This is because the triangular crystal is enthalpically more favored at any positive pressure since there is no energy penalty associated with the formation of triangular crystal, and the triangular crystal is denser than the kagomé crystal. We also try four variable-sized patches centered at the angles consistent with the tetravalent coordination of this crystal, and the resulting structures are dense triangular crystal as well. These results suggest that additional interactions are required to prohibit the triangular lattice from being a competitor. We note that in the experimental work,[28] additional electrostatic repulsions between equator portions of the particles are indeed mentioned. This prompts us to incorporate additional directional repulsion into our potential.

Specifically, we consider

$$u_2(\mathbf{r}_{ij}) = \begin{cases} \infty, & \text{if } r_{ij} < \sigma, \text{ or} \\ & \sigma < r_{ij} < \lambda_r\sigma, \ \hat{\mathbf{n}}_i\cdot\hat{\mathbf{r}}_{ij} \le \cos\theta \\ & \text{and } \hat{\mathbf{n}}_j\cdot\hat{\mathbf{r}}_{ji} \le \cos\theta \\ -\varepsilon, & \text{if } \sigma < r_{ij} < \lambda_a\sigma, \ \hat{\mathbf{n}}_i\cdot\hat{\mathbf{r}}_{ij} \ge \cos\theta \\ & \text{and } \hat{\mathbf{n}}_j\cdot\hat{\mathbf{r}}_{ji} \ge \cos\theta \\ 0, & \text{otherwise} \end{cases} \quad (5)$$

where λ_a, λ_p are the radial ranges of the directional attraction between patches and repulsion between equator portions of the particles, respectively, and the definitions of other parameters are the same as those in eq 4. This directional pair interaction is illustrated in Figure 4. We employ two identical patches equally spaced on the surface of each particle and perform simulated annealing of a system with $N = 48$ particles. We find that when λ_a

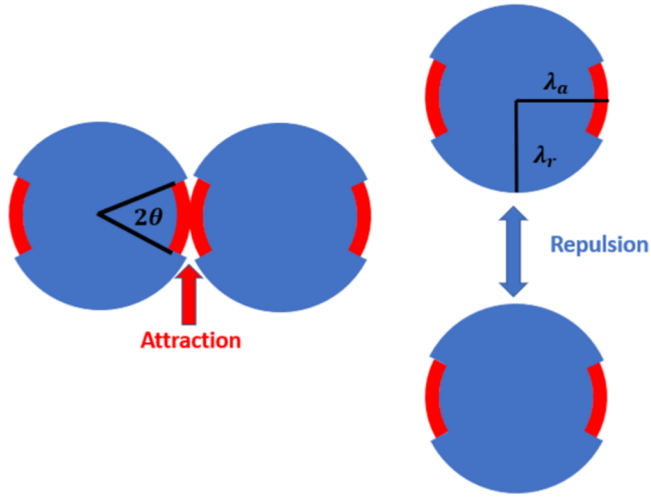

Figure 4. Illustration of the patchy interactions given by eq 5, where the repulsive and attractive regions of the particles are colored blue and red, respectively. Two particles experience attraction when they approach each other in angles within the angular range of the patches and hard repulsion when they approach each other through surfaces not covered by patches. The angular width and radial range of the patches are given by 2θ and λ_a, respectively, and the radial range of the directional hard repulsion is given by λ_r.

= 1.10, $\lambda_r = 1.50$, $\cos\theta = 0.84$, and $p = 1.50$, the particles self-assemble into a perfect kagomé lattice, as shown in Figure 5a. The corresponding effective packing fraction of the colloids ϕ is 0.64. This example shows that open low-density crystal structures may not necessarily be achieved with only very short-ranged patchy attractions at the obvious coordination sites. This issue may be especially important in three dimensions for highly symmetric crystals. However, for low-density three-dimensional targets with low symmetry, such as the tunneled crystals,[42] optimally placed patches may be sufficient to achieve such open crystals via self-assembly, although this remains an open question. This is because in these cases, the arrangement of patches prohibits the hexagonal-close-packed or face-centered-cubic crystals from being competitors at intermediate pressures, as these dense crystals are energetically unfavorable.

Besides the kagomé crystal, we also attempt to obtain parallelogrammic crystal through the inverse design of the type of potential described in eq 5. Specifically, our goal is to obtain a parallelogrammic crystal with lattice parameters $b/a = 1.30$ and $\alpha = 67°$, where a and b are the lengths of the two lattice vectors, and α is the angle between the two lattice vectors. We employ $N = 36$ particles, with two patches equally spaced on the surface of each particle. Through similar procedures as those for the kagomé crystal, we find that when $\lambda_a = 1.05$, $\lambda_r = 1.30$, $\theta = \pi/12$, and $p = 1.50$, the particles self-assemble into a perfect parallelogrammic crystal, as shown in Figure 5b. The corresponding effective packing fraction of the colloids ϕ is 0.61.

In addition, we investigate how sensitive the self-assembly is to deviations of the pressure from the targeted value. We find that for all of the systems studied, the resulting structures are very similar (except for a slight change in the number of defects) when the pressure varies by as much as 25% around the target value, implying the robustness of our results. This bodes well for their experimental realization. Moreover, we find that the optimal parameter values determined in this work for the self-assembly of the target square and honeycomb crystals are

DOI: 10.1021/acs.jpcb.8b05627
J. Phys. Chem. B 2018, 122, 8462−8468

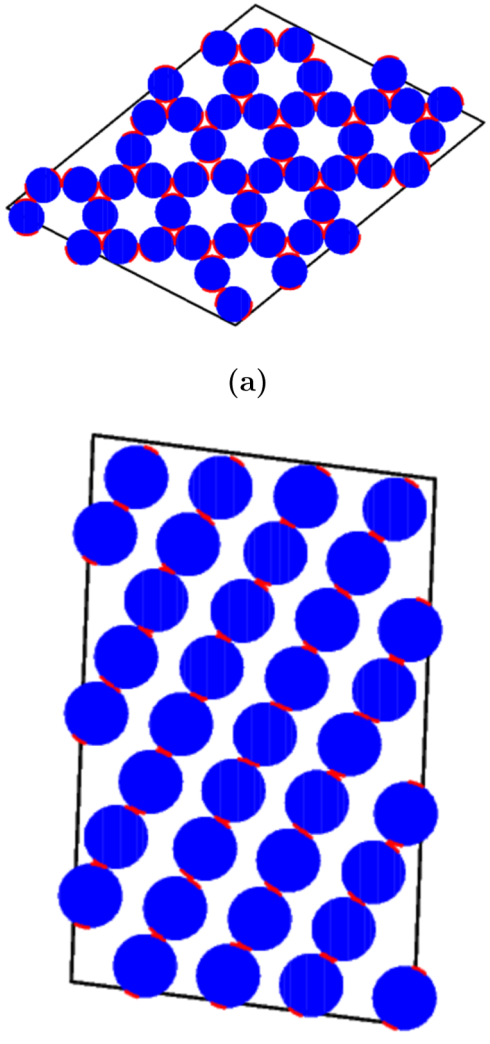

Figure 5. (a) Self-assembly of perfect kagomé lattice by particles with directional repulsions and two attractive equally-spaced patches over each particle, as described by eq 5. The optimized parameters are found to be $\lambda_a = 1.10$, $\lambda_r = 1.50$, $\cos\theta = 0.84$, and $p = 1.50$. (b) Self-assembly of perfect parallelogrammic lattice by particles with directional repulsions and two attractive equally-spaced patches over each particle, as described by eq 5. The optimized parameters are found to be $\lambda_a = 1.05$, $\lambda_r = 1.30$, $\theta = \pi/12$, and $p = 1.50$.

consistent with those reported in a previous forward study for these crystals.[27]

IV. CONCLUSIONS AND DISCUSSION

In this work, we employed the inverse statistical mechanics approach to determine optimized patchy interactions that enable the robust self-assembly of relatively defect-free low-coordinated crystals in two dimensions at fixed pressure and sufficiently low temperatures, including square, honeycomb, kagomé, and parallelogrammic crystals. Note that suboptimal parameters not only increase the number of defects, but also may lead to a completely different structure, like the triangular lattice. We found that although isotropic hard-core repulsion and directional attraction between patches were sufficient for the formation of square and honeycomb crystals, an additional directional repulsion beyond the hard cores were needed for the formation of kagomé and parallelogrammic crystals.

Our computational findings provide optimal parameters to experimentalists to synthesize these crystals using standard techniques[28,43−46] and laboratory conditions while being robust with respect to pressure changes from the target pressure value. This strongly suggests that our targeted structures should be straightforward to achieve in the laboratory. In particular, the directional repulsion between particles in the cases of kagomé and parallelogrammic crystals can be realized in experiments by ionizing certain portions of the particle surface and creating net surface charges.[28]

Although we focused on targeting several different 2D crystals here, the same inverse approach can be generalized to design optimized patchy potentials for a variety of more complex structures in two dimensions, as discussed in a previous work[27] (e.g., zigzag lanes) as well as nontrivial targets in three dimensions, e.g., pyrochlore crystals, which possess useful photonic properties.[8] Importantly, it is highly desirable in a future work to identify an appropriate objective function and develop a full-blown optimization technique for the inverse design of anisotropic patchy interactions for various target crystals, including those studied in this work. Such a new technique will be much more efficient and preclude the use of visual inspection in the current optimization algorithm that discretely searches the parameter space.

It is instructive to point out the differences between our inverse approach and previous conventional forward studies of patchy particles.[47−50] Those forward studies generally focused on the investigation of the phase diagrams of certain parameterized potentials, and the resulting structures are not known a priori. Our goal, on the other hand, is to obtain relatively defect-free target crystals that are known a priori by optimizing the parameters via a multistage grid-search approach. Moreover, in those forward studies of patchy particles, the parameter values are usually evenly distributed in the parameter space, and there is no real parameter optimization process in an inverse manner, even in a coarse sense. This is consistent with their goal of determining the phase diagrams for a given potential and is distinctly different from our inverse approach. Nonetheless, it would be interesting to study the full phase diagrams of the potentials that have been identified in this work (including parameter ranges that were not investigated in this work). This is especially the case for the potentials that involve directional repulsions and attractions that we employed to obtain kagomé and parallelogrammic crystals. A natural extension of our work is the investigation of the exotic structures that may emerge in colloidal systems with short-ranged directional attractions and longer-ranged isotropic radial repulsions.[51]

AUTHOR INFORMATION

Corresponding Author

*E-mail: torquato@electron.princeton.edu.

ORCID

S. Torquato: 0000-0003-4614-335X

Notes

The authors declare no competing financial interest.

DOI: 10.1021/acs.jpcb.8b05627
J. Phys. Chem. B 2018, 122, 8462−8468

■ ACKNOWLEDGMENTS

We thank Francesco Sciortino for helpful discussions. This work was supported by the National Science Foundation under Award No. CBET-1701843.

■ REFERENCES

(1) Rechtsman, M. C.; Stillinger, F. H.; Torquato, S. Optimized interactions for targeted self-assembly: Application to a honeycomb lattice. *Phys. Rev. Lett.* **2005**, *95*, No. 228301.
(2) Rechtsman, M. C.; Stillinger, F. H.; Torquato, S. Designed interaction potentials via inverse methods for self-assembly. *Phys. Rev. E* **2006**, *73*, No. 011406.
(3) Rechtsman, M. C.; Stillinger, F. H.; Torquato, S. Self-assembly of the simple cubic lattice with an isotropic potential. *Phys. Rev. E* **2006**, *74*, No. 021404.
(4) Weeks, J. D.; Chandler, D.; Andersen, H. C. Role of repulsive forces in determining the equilibrium structure of simple liquids. *J. Chem. Phys.* **1971**, *54*, 5237.
(5) Watzlawek, M.; Likos, C. N.; Löwen, H. Phase diagram of star polymer solutions. *Phys. Rev. Lett.* **1999**, *82*, 5289−5292.
(6) Prestipino, S.; Saija, F.; Malescio, G. The zero-temperature phase diagram of soft-repulsive particle fluids. *Soft Matter* **2009**, *5*, 2795−2803.
(7) Levashov, V. A. Crystalline structures of particles interacting through the harmonic-repulsive pair potential. *J. Chem. Phys.* **2017**, *147*, No. 114503.
(8) Pattabhiraman, H.; Avvisati, G.; Dijkstra, M. Novel Pyrochlorelike Crystal with a Photonic Band Gap Self-Assembled Using Colloids with a Simple Interaction Potential. *Phys. Rev. Lett.* **2017**, *119*, No. 157401.
(9) Rechtsman, M. C.; Stillinger, F. H.; Torquato, S. Synthetic diamond and wurtzite structures self-assemble with isotropic pair interactions. *Phys. Rev. E* **2007**, *75*, No. 031403.
(10) Rechtsman, M. C.; Stillinger, F. H.; Torquato, S. Negative thermal expansion in single-component systems with isotropic interactions. *J. Phys. Chem. A* **2007**, *111*, 12816−12821.
(11) Rechtsman, M. C.; Stillinger, F. H.; Torquato, S. Negative Poisson's ratio materials via isotropic interactions. *Phys. Rev. Lett.* **2008**, *101*, No. 85501.
(12) Marcotte, É.; Stillinger, F. H.; Torquato, S. Optimized monotonic convex pair potentials stabilize low-coordinated crystals. *Soft Matter* **2011**, *7*, 2332−2335.
(13) Marcotte, É.; Stillinger, F. H.; Torquato, S. Unusual ground states via monotonic convex pair potentials. *J. Chem. Phys.* **2011**, *134*, No. 164105.
(14) Jain, A.; Errington, J. R.; Truskett, T. M. Inverse design of simple pairwise interactions with low-coordinated 3D lattice ground states. *Soft Matter* **2013**, *9*, 3866−3870.
(15) Jain, A.; Errington, J. R.; Truskett, T. M. Dimensionality and design of isotropic interactions that stabilize honeycomb, square, simple cubic, and diamond lattices. *Phys. Rev. X* **2014**, *4*, No. 031049.
(16) Marcotte, É.; Stillinger, F. H.; Torquato, S. Designed Diamond Ground State via Optimized Isotropic Monotonic Pair Potentials. *J. Chem. Phys.* **2013**, *138*, No. 061101.
(17) Zhang, G.; Stillinger, F. H.; Torquato, S. Probing the limitations of isotropic pair potentials to produce ground-state structural extremes via inverse statistical mechanics. *Phys. Rev. E* **2013**, *88*, No. 042309.
(18) Chen, D.; Aw, W. Y.; Devenport, D.; Torquato, S. Structural characterization and statistical-mechanical model of epidermal patterns. *Biophys. J.* **2016**, *111*, 2534−2545.
(19) Piñeros, W. D.; Baldea, M.; Truskett, T. M. Designing convex repulsive pair potentials that favor assembly of kagome and snub square lattices. *J. Chem. Phys.* **2016**, *145*, No. 054901.
(20) Piñeros, W. D.; Jadrich, R. B.; Truskett, T. M. Design of two-dimensional particle assemblies using isotropic pair interactions with an attractive well. *AIP Adv.* **2017**, *7*, No. 115307.
(21) Chao, H.; Riggleman, R. A. Inverse design of grafted nanoparticles for targeted self-assembly. *Mol. Syst. Des. Eng.* **2018**, *3*, 214−222.
(22) Escobedo, F. A. Optimizing the formation of colloidal compounds with components of different shapes. *J. Chem. Phys.* **2017**, *147*, No. 214501.
(23) Kern, N.; Frenkel, D. Fluid-fluid coexistence in colloidal systems with short-ranged strongly directional attraction. *J. Chem. Phys.* **2003**, *118*, 9882−9889.
(24) Sear, R. P. Interactions in protein solutions. *Curr. Opin. Colloid Interface Sci.* **2006**, *11*, 35−39.
(25) Pawar, A. B.; Kretzschmar, I. Patchy particles by glancing angle deposition. *Langmuir* **2008**, *24*, 355−358.
(26) Pawar, A. B.; Kretzschmar, I. Multifunctional patchy particles by glancing angle deposition. *Langmuir* **2009**, *25*, 9057−9063.
(27) Doppelbauer, G.; Bianchi, E.; Kahl, G. Self-assembly scenarios of patchy colloidal particles in two dimensions. *J. Phys.: Condens. Matter* **2010**, *22*, No. 104105.
(28) Chen, Q.; Bae, S. C.; Granick, S. Directed self-assembly of a colloidal kagome lattice. *Nature* **2011**, *469*, 381−384.
(29) Romano, F.; Sciortino, F. Two dimensional assembly of triblock Janus particles into crystal phases in the two bond per patch limit. *Soft Matter* **2011**, *7*, 5799−5804.
(30) Saika-Voivod, I.; Smallenburg, F.; Sciortino, F. Understanding tetrahedral liquids through patchy colloids. *J. Chem. Phys.* **2013**, *139*, No. 234901.
(31) Romano, F.; Sciortino, F. Patterning symmetry in the rational design of colloidal crystals. *Nat. Commun.* **2012**, *3*, No. 975.
(32) Smallenburg, F.; Leibler, L.; Sciortino, F. Patchy particle model for vitrimers. *Phys. Rev. Lett.* **2013**, *111*, No. 188002.
(33) Couny, F.; Benabid, F.; Light, P. S. Large-pitch kagome-structured hollow-core photonic crystal fiber. *Opt. Lett.* **2006**, *31*, 3574−3576.
(34) Rechtsman, M. C.; Jeong, H.-C.; Chaikin, P. M.; Torquato, S.; Steinhardt, P. J. Optimized structures for photonic quasicrystals. *Phys. Rev. Lett.* **2008**, *101*, No. 073902.
(35) Mohammadi, S.; Eftekhar, A. A.; Khelif, A.; Moubchir, H.; Westafer, R.; Hunt, W. D.; Adibi, A. Complete phononic bandgaps and bandgap maps in two-dimensional silicon phononic crystal plates. *Electron. Lett.* **2007**, *43*, 898−899.
(36) Atwood, J. L. Kagome lattice: a molecular toolkit for magnetism. *Nat. Mater.* **2002**, *1*, 91.
(37) Rowan, T. H. Functional Stability Analysis of Numerical Algorithms. Ph.D. Thesis, Department of Computer Sciences; University of Texas at Austin, 1990.
(38) Shin, H.; Schweizer, K. S. Theory of two-dimensional self-assembly of Janus colloids: crystallization and orientational ordering. *Soft Matter* **2014**, *10*, 262−274.
(39) Iwashita, Y.; Kimura, Y. Orientational order of one-patch colloidal particles in two dimensions. *Soft Matter* **2014**, *10*, 7170−7181.
(40) Iwashita, Y.; Kimura, Y. Spatial confinement governs orientational order in patchy particles. *Sci. Rep.* **2016**, *6*, No. 27599.
(41) Nourani, Y.; Andresen, B. A comparison of simulated annealing cooling strategies. *J. Phys. A: Math. Gen.* **1998**, *31*, 8373.
(42) Torquato, S.; Stillinger, F. H. Toward the jamming threshold of sphere packings: Tunneled crystals. *J. Appl. Phys.* **2007**, *102*, No. 093511.
(43) Wang, Y.; Wang, Y.; Breed, D. R.; Manoharan, V. N.; Feng, L.; Hollingsworth, A. D.; Weck, M.; Pine, D. J. Colloids with valence and specific directional bonding. *Nature* **2012**, *491*, 51.
(44) Yi, G.-R.; Pine, D. J.; Sacanna, S. Recent progress on patchy colloids and their self-assembly. *J. Phys.: Condens. Matter* **2013**, *25*, No. 193101.
(45) Gong, Z.; Hueckel, T.; Yi, G.-R.; Sacanna, S. Patchy particles made by colloidal fusion. *Nature* **2017**, *550*, 234.
(46) Ravaine, S.; Duguet, E. Synthesis and assembly of patchy particles: Recent progress and future prospects. *Curr. Opin. Colloid Interface Sci.* **2017**, *30*, 45−53.
(47) Vissers, T.; Preisler, Z.; Smallenburg, F.; Dijkstra, M.; Sciortino, F. Predicting crystals of Janus colloids. *J. Chem. Phys.* **2013**, *138*, No. 164505.

DOI: 10.1021/acs.jpcb.8b05627
J. Phys. Chem. B 2018, 122, 8462−8468

(48) Munaò, G.; Preisler, Z.; Vissers, T.; Smallenburg, F.; Sciortino, F. Cluster formation in one-patch colloids: low coverage results. *Soft Matter* **2013**, *9*, 2652−2661.
(49) Preisler, Z.; Vissers, T.; Smallenburg, F.; Munaò, G.; Sciortino, F. Phase diagram of one-patch colloids forming tubes and lamellae. *J. Phys. Chem. B* **2013**, *117*, 9540−9547.
(50) Preisler, Z.; Vissers, T.; Munaò, G.; Smallenburg, F.; Sciortino, F. Equilibrium phases of one-patch colloids with short-range attractions. *Soft Matter* **2014**, *10*, 5121−5128.
(51) Yigit, C.; Heyda, J.; Dzubiella, J. Charged patchy particle models in explicit salt: ion distributions, electrostatic potentials, and effective interactions. *J. Chem. Phys.* **2015**, *143*, No. 064904.

DOI: 10.1021/acs.jpcb.8b05627
J. Phys. Chem. B 2018, 122, 8462−8468